STUDIES ON ISOTHERM MODELING OF BASIC GREEN 4 ADSORPTION BY NOVEL FIRECLAY-MnO_2 NANOCOMPOSITE ADSORBENT

Rathinavelu[1], P.Balasubramaniam[2],V.Venkateswaran[3]
[1,2] Department of Chemistry, [3] Dean, Physical Sciences, [1,2]Erode Arts and Science College, Erode-638009, Tamilnadu, India
,[3]Sree Saraswathi Thyagaraja College, Pollachi-642107,Tamilnadu, India

Abstract

Nano composite based on fireclay and manganese dioxide was synthesized by typical sol-gel method and utilized as the potential adsorbent for the adsorption of Basic Green 4 from aqueous system. Characterization was carried by Scanning Electron Microscopy (SEM), Fourier Transform Infra-red Spectroscopy (FTIR) and X-ray Diffraction (XRD) Analysis. Adsorptive capability was evaluated using batch adsorption experiments with specific reference to particle size, pH and Temperature. The experimental data were fitted with different isotherm models such as Langmuir, Freundlich, Temkin, Dubinin-Radushkevich and Halsey and found well fitted with Langmuir isotherm model showing maximum adsorption capacity of 76.41mg/g. This fitness of the isotherm was assessed based on r^2 values and error analysis.

Keywords: Nanocomposite : Basic Green 4; Isotherm Models; Adsorption

I. Introduction

The development of new materials [1] and methods for reducing color in textile effluent streams in recent years has led in to new insights in this field[2-3]. Clay varieties such as smectites (montmorillonite and saponite), mica (illite), kaolinite, serpentine, pylophyllite (talc), vermiculite and sepiolite [4] and new polymer-clay nanocomposites were developed as low cost adsorbents for nonionic and anionic pollutants [5], organic pollutants [6], anionic herbicides [7], atrazine [8], etc.

In nanocomposites, nanoparticles (clay, metal, carbon nanotubes, etc.) act as fillers in a matrix. Nanoparticles are particles of less than 100 nm in diameter that exhibit new or enhanced size-dependent properties compared to the larger particles of the same material. Clay nanocomposites are the materials in which major component of the material, clay is in combination with other materials like metals, polymer, and so forth [9]. MnO_2 is a well-known solid-phase oxidant that exists in different forms [10-11] with a high oxidation potential. Familiar minerals in the natural environments are iron and manganese oxides, which have relatively high surface areas and surface charges. They often regulate free metal and organic matter concentration in soil or water through adsorption reactions. Many researchers have utilized iron and manganese oxides for the removal of heavy metals and organic matter in water by adsorption.

Adsorption equilibria provide the most important information for understanding the adsorption process. Regardless of how many components are present in the system, the adsorption equilibria and diffusion of pure components are very essential for understanding the amount of those components which can be accommodated by a solid adsorbent [12-13]. Modeling of sorption isotherm data is important for predicting and comparing the adsorption performance. Two-parameter isotherm models are available for modeling adsorption data. Langmuir [14], Freundlich [15]models are the most commonly used isotherms. Further other models such as Temkin [16-17] Dubinin- Radushkevich [18-19], Halsey [20] were also used.

In this paper, results of the studies on the use of fireclay and its composite, an ecofriendly efficient adsorbent, for the removal of wastewater contaminant Basic Green 4 from simulated wastewater are presented and discussed. Various isotherm equations were used to assess the best isotherm equation which fits the experimental data satisfactorily.

II. Materials and Methods

a) Synthesis of Nanocomposite

Fire clay (3 g) was allowed to swell in 15 mL of alcohol and stirred for 2 hours at 25 °C to get a uniform suspension. At the same time, the MnO_2 was dispersed into alcohol. The diluted manganese dioxide was then added slowly by dropping it in the suspension of Fire clay and stirred for further 5 hours at 25 °C. Then 5 mL alcohol mixed with 0.2 mL deionized water was added slowly and stirring continued for another 5 hours at 25 °C. The suspension was then kept overnight for 10 hours at room temperature and the precipitate obtained was carefully dehydrated in a vacuum oven for 6 hours at 80 °C to get an amorphous dry powder. A stock solution (1000 mg/L) of Basic Green 4 dye was prepared using doubly distilled water. Various concentrations of the dye solution were prepared by diluting the stock dye solution.

b) Batch Adsorption Experiments

Surface morphology of the nanocomposite was studied by using SEM and XRD studies. Batch mode experiments were carried out at three different temperatures 303 K, 318K and 333 K by taking 50 mL of the respective dye solution and 50 mg of the adsorbent in a 100 mL Erlenmeyer flask. The flasks were agitated for pre-determined time intervals in a thermostat attached with a shaker at the desired temperature. The adsorbent was separated by centrifugation and the absorbance was measured using Elico (SL 210) UV-Visible spectrometer. Studies on the effects of agitation time, pH and temperature were carried out by using known amount of adsorbent and 50mL of dye solution of different concentrations.

III. Results and Discussions

3.1. Characterization of the adsorbent

Figure 1 a and b shows the XRD patterns of pure fireclay and that of fire clay- MnO_2 nanocomposite respectively. The peaks at $2\theta = 27.2°$(Figure 1a & b) confirm the presence of fireclay MnO_2 phase in the nanocomposite.

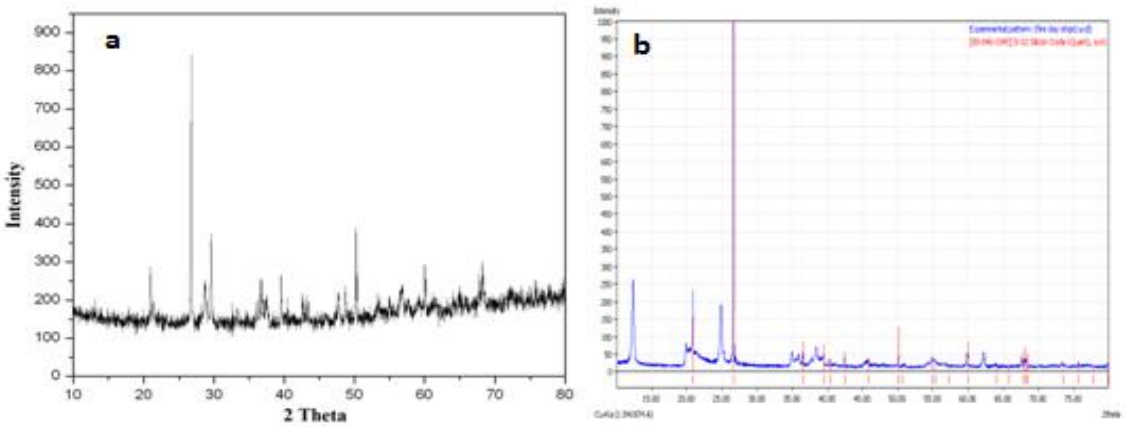

Fig. 1 a & b. XRD pattern of pure fireclay and fireclay-MnO_2 nanocomposite

The major and minor peaks for fireclay and fireclay MnO_2 samples were obtained at 2θ values 21, 27.2, 36.16, 50 and 60° which represents the presence of crystalline planes. The spinel peaks and narrower peaks indicate the amorphous and crystalline nature of both fireclay and fireclay-MnO_2 nanocomposite. Further the band observed at $2\theta = 43.6°$, which is attributed to graphite-like atomic order within a single plane, is indicative of the graphitization [21].

The surface morphology of the adsorbent was visualized via scanning electron microscopy (SEM). The diameter of the pure fire clay range was 20µm (Fig.2a) and that of fire clay- MnO_2 composite was 0.5µm. (Fig2b). The nanocomposite showed a characteristic pore size depending on the starting material used. The micro porous nanocomposite obtained from the pure fireclay material and MnO_2 are more effective to retain little molecules on contrary to amorphous nanocomposite. The amorphous structure of the nanocomposite is responsible for the transport and adsorption of the large dye molecules.

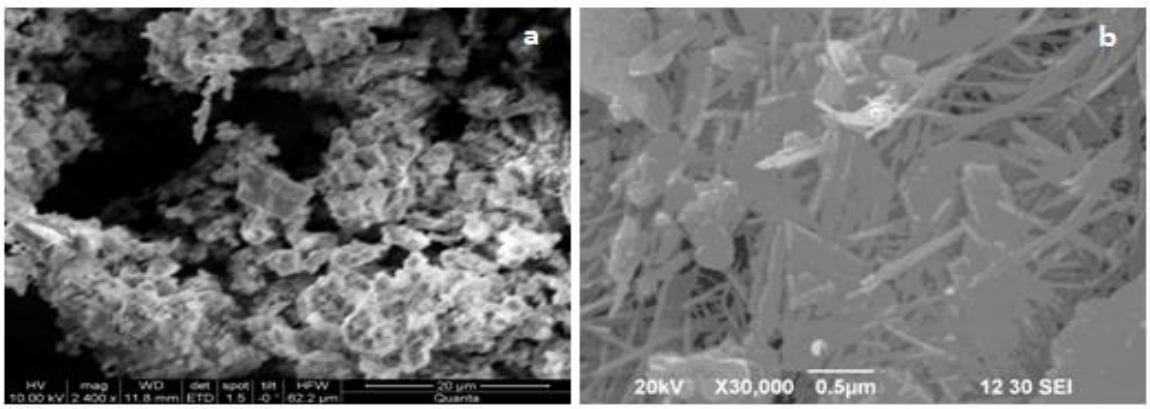

Fig. 2 a & b. SEM images of pure fireclay and fireclay-MnO_2 nanocomposite

Fourier Transform Infra-Red (FTIR) Transmission spectra were obtained to characterize the functional groups in the fireclay and fireclay nanocomposite. Figure 3 a and 3b shows the FTIR spectra of fireclay and fireclay-MnO_2 nanocomposite. The fireclay and MnO_2 contains more bands than the nanocomposite. The peaks at wave number 3693.09Cm^{-1} and 1209.72 Cm^{-1} indicate the presence of $–CH_2$ and -CH stretching. The absorption peaks at wave numbers less than 1000 cm^{-1} in both the spectra confirm the presence of transition metal ions in the nanocomposite material.

Fireclay: –CH_2 stretching= 3693.09 cm^{-1}, -CH stretching = 1209.72cm^{-1}, Si–O bond = 1011.17 cm^{-1}, Si -O- Mn = 766.37cm^{-1}.

Fireclay+MnO_2 NC: –CH_2 stretching = 3723. 07 cm^{-1}, -CH stretching = 1383.83cm^{-1}, Si-O = 966.61 cm^{-1}, Mn -O- Mn = 522.29 cm^{-1}.

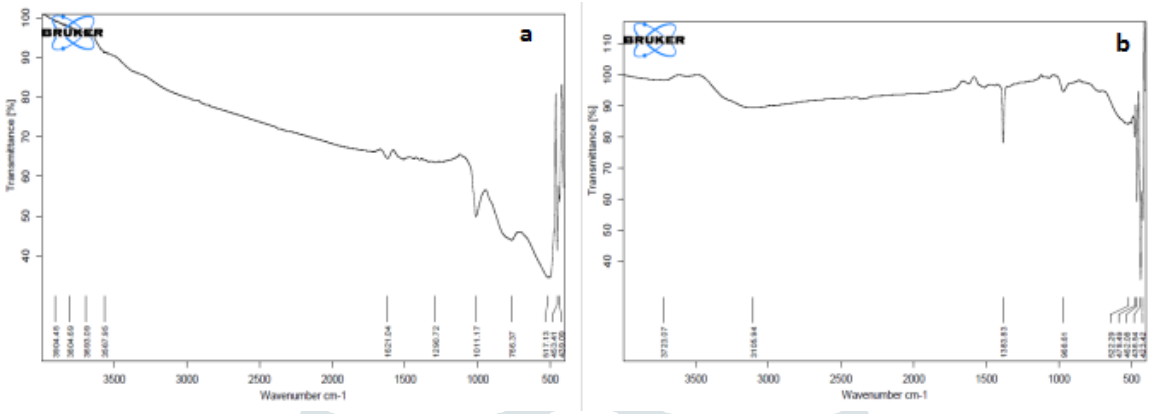

Fig. 3 a & b. FTIR image of pure fireclay and fireclay-MnO_2 nanocomposite

3.2. Isotherm Studies

The adsorption isotherm describes the interaction of adsorbates with adsorbents and therefore it is critical in optimizing the use of adsorbents.

The applicability of the isotherm equation is compared by judging the correlation coefficients (R^2). The Langmuir, Freundlich models are often used to describe equilibrium adsorption isotherms and Temkin, Dubinin-Radushkevich and Halsey models are also applied to describe equilibrium sorption isotherms. Different isotherm models used in this study are given Table 1.

Table 1 *List of adsorption isotherm models used for this study*

Model	Formula	Reference
Langmuir	$q_e = Q_m \frac{K_L C_e}{1 + K_L C_e}$	[17]
Freundlich	$q_e = K_F C_e^{1/n}$	[18]
Temkin	$q_e = \ln K_T C_e$	[19-20]
Halsey	$q_e = [A_{HJ}/B_{Hj} \log C_e)]^{1/2}$	[25]
Dubinin- Radushkevich	$q_e = q_{DR} \exp(-K_{DR}^2)$	[26]

Adsorption isotherm modeling is also adopted for Basic green 4 adsorptions onto Fireclay nanocomposite. The Langmuir equation is valid for monolayer sorption onto a surface with a finite number of identical sites. The theoretical and experimental data for the application of Langmuir model are shown in Table 2. The values of maximum adsorption capacity determined using Langmuir model was 48.35, 66.95 and 76.41mg/g at 30, 45 and 60°C temperatures respectively. These theoretical values are nearly equal to the experimental data and correspond closely to the adsorption isotherm plateau, which are within acceptable limits.

Table 2 *Different isotherm rate constant parameters for the adsorption of Basic Green 4 onto fireclay-MnO_2 nanocomposite*

Model	**Isotherm Constants**	**Basic Green 4**		
		30 °C	**45 °C**	**60 °C**
Langmuir	Q_0(mg g^{-1})	48.35	66.95	76.41
	K_L(L mg^{-1})	0.0462	0.0470	0.0530
	R^2	0.9922	0.9928	0.9895
Freundlich	n	2.0729	1.9596	1.9314
	K_f(mg g^{-1})(L $mg^{-1})^{1/n}$	4.6546	5.9377	6.9651

	R^2	0.9244	0.9194	0.9227
Temkin	β_T(KJ mol^{-1})	10.4689	14.3970	16.4716
	α_T(L mg^{-1})	0.4660	0.4892	0.5481
	R^2	0.9687	0.9716	0.9599
Halsey	K_h(mg g^{-1})	24.2369	32.8109	42.4658
	N	2.0729	1.9596	1.9314
	R^2	0.8944	0.9194	0.9227
D-R	K-DR(mol^2 KJ^{-2})	11.05E-06	6.886E-05	4.699E-05
	Q_m(mg g^{-1})	33.09	42.45	47.31
	R^2	0.7957	0.7500	0.7056
	E	0.0052	0.0041	0.00342

The essential characteristics of the Langmuir isotherm can be expressed in terms of dimensionless separation factor or equilibrium parameter, R_L [22], defined as

$$R_L = \frac{1}{1 + bC_0}$$

where b is the Langmuir constant and C_0 (mg L^{-1}) is the highest initial dye concentration respectively.

The values of dimensionless separation factors (R_L) for adsorption of Basic green 4 on fireclay-MnO_2 nanocomposite were less than 1 and greater than 0 indicating a favorable adsorption.

The Freundlich equation an empirical relation, is based on sorption onto a heterogeneous surfaces. The magnitude of exponent 'n' gives an indication on the favorability of adsorption. It is generally stated that the values n greater than 1 indicate a favourable adsorption[23].The intensity (n) of adsorption gives an indication of the bond energies between dye and adsorbent and the possibility of slight chemisorption rather than physisorption [24]. Since the values of n are greater than one the possibility of multilayer adsorption of dye through the percolation process cannot be ruled out [25].

However, the Langmuir isotherm shows (Figure 4a) a better fit to the adsorption data than the Freundlich isotherm for the sorption of Basic green 4. Such a trend is quite logical since the Freundlich equation is a pure exponential one, which means that when $C_e\infty$, q_e will also extend to ∞ [26]. However, for all dyes adsorption systems, since there is a clear saturation plateau, the calculated q_e will necessarily tend towards a maximum (i.e. maximum adsorption capacity). The fact that the Langmuir isotherm fits the experimental data well may be predominantly due to the homogeneous distribution of active sites on the activated carbon surface[17]. The plots for Freundlich isotherm shown in (Figure 4b) and the value of Freundlich constants, n (2.0729, 1.9596 and 1.9314) indicate favorable adsorption. The comparison of Basic green 4 adsorption capacities on fireclay-MnO_2 nanocomposite at different temperatures was given in Table 6.

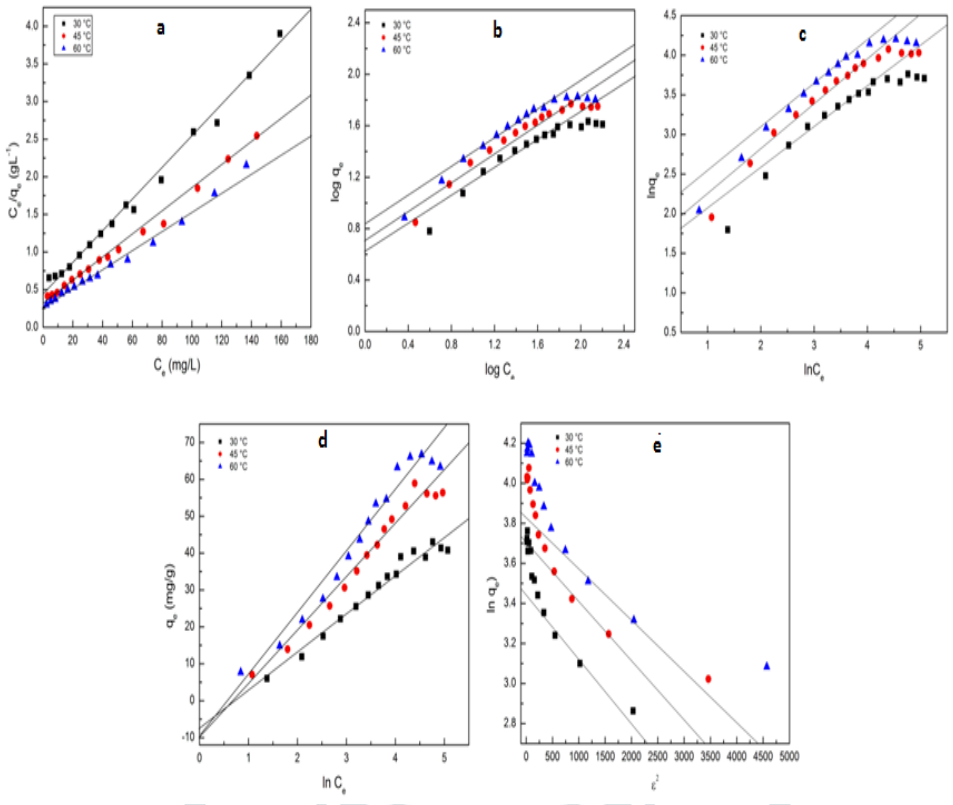

Figure 4 a,b,c,d and e *Langmuir, Freundlich, Halsey, Temkin and DR Isotherm plot for the adsorption of Basic Green 4 onto fireclay – MnO_2 nanocomposite at various temperatures*

Temkin and Pyzhev [27-28] studied the heat of adsorption and the adsorbent–adsorbate interaction on surfaces. The Temkin isotherm plot was given in figure 4d. The variation of adsorption energy was very low and positive showing that the adsorption process may be physisorption and endothermic in nature [29]. This model assumes that the heat of adsorption (function of temperature) of all molecules in the layer would decrease straightly with coverage when the lowest and the highest values of concentration are ignored [33].

The Halsey [30] adsorption isotherm is suitable for multilayer adsorption and the fitting of the experimental data to this equation indicate the heteroporous nature of the adsorbent. Relatively poor agreement was found for the Halsey model with the experimental data. The Halsey isotherm plots were represented in Figure 4c at three different temperatures.

Dubinin-Radushkevich (D-R) isotherm model can predict good results at low concentration ranges and the model may be applied to explain the adsorption on both homogeneous and heterogeneous surfaces [18-19 & 31]. The plots were show in figure 4e. The constant, BD, is related to the mean free energy of sorption per mole of the sorbate as it is transferred to the surface of the solid from an infinite distance in the solution. Though D-R is an empirical model, it attempts to differentiate the physical and chemical adsorption for the removal of effluents [32] with the mean free energy (E) value. The value of E (kJ/mol) is very useful in predicting the type of adsorption, i.e, whether the adsorption process under study is physical or chemical in nature. It is predicted that when the value of E is less than 8 kJ/mol, the adsorption is said to be physical while if it is in between 8-16 kJ/mol, then the adsorption is said to be chemical in nature [33]. It can be observed from Table 2 that the mean free energy (E) values are 0.0052, 0.0041 and 0.0034 kJ/mol. This indicates that physisorption plays a significant role in adsorption and there will be no possibility of chemisorption. Because in this case of physical adsorption, while increasing the temperature of the system, the extent of dye adsorption increase.

3.3. Error Analysis and Statistics

In order to analyze the impact of various error functions on the predicted isotherms, various error functions and statistics like HYBRID, MPSD, ARE, SSE, EABS, F test, RMSE, $\chi 2$ test and G^2 test were examined and in each case, the isotherm parameters were determined by minimizing the respective error function across the concentration range studied, using the solver add-in for Microsoft Excel. The expressions of various error functions used in the present study are given in Table 3.

Langmuir and Freundlich isotherm show a satisfactory fit to the experimental data as indicated by the values of RMSE and χ^2. However, the Langmuir isotherm showed a better fit to adsorption data than Freundlich isotherm. The fact that the Langmuir isotherm fits the experimental data well may be due to homogeneous distribution of active sites on the Fireclay nanocomposite surface [14]. As shown, the Freundlich isotherm has a second satisfactory fit to the experimental data as indicated by the error functions [34]. In Freundlich isotherm the χ^2 square value was greater than G^2 values as shown in Table 4&5.

The obtained results (Table 2,4 & 5) for Basic green 4 showed that the best fitted adsorption isotherm models were in the order Langmuir>Temkin>Freundlich>Halsey>Dubinin-Radushkevich on the basis of high R^2 values. The root mean square value, lower χ^2 and SSE were obtained in the order of Langmuir>Freundlich>Halsey>Dubinin-Radushkevich>Temkin. The lower value the SSE, RMSE and χ^2 shows a best fit for Langmuir isotherm first and then for Freundlich for the adsorption of Basic green 4 onto fireclay nanocomposite.

Table 3 *list of error functions and statistics used for this study*

Error Function	Expression	Reference
The sum of the squares of the errors (SSE):	$\sum (q_{e,cal} - q_{e,exp})^2$	[35]
Average relative error (ARE)	$\frac{1}{N}\sum (\frac{q_{e,cal} - q_{e,exp}}{q_{e,exp}}) 100$	[36]
Marquardt's percent standard deviation (MPSED)	$\sqrt{\frac{\sum (q_{e,exp} - q_{e,cal})^2}{N - P}} 100$	[36]
The hybrid fractional error function (HYBRID)	$\frac{1}{N - P}\sum \left[\frac{q_{e,cal} - q_{e,exp})}{q_{e,exp}}\right] 100$	[36]
Residual Root Mean Square Error (RMSE)	$\sum \frac{1}{N - 2}\sum_{i=1}^{n} (q_{e,exp} - q_{e,cal})^2$	[34]
Chi Square (χ^2)	$\sum_{i=1}^{n} \frac{(q_{e,exp} - q_{e,cal})^2}{q_{e,exp}}$	[34]
Akaike Information Criterion (AIC_C)	$AIC + \frac{2P(P+1)}{N - 1 - P}$	[34]
Log-likelihood test (G^2)	$2\sum_{i=1}^{n} [q_{e,exp} \text{ x } \ln \frac{q_{e,exp}}{q_{e,cal}}]$	[34]
The sum of Absolute Error (EABS)	$\sum \lvert q_{e,cal} - q_{e,exp} \rvert^2$	[35]

Table 4 *Different error function parameters for the adsorption of Basic Green 4 onto fireclay-MnO_2 nanocomposite material*

Model	Error Functions	Basic Green 4		
		30 °C	45 °C	60 °C
Langmuir	SSE	0.1138	0.0451	0.0443
	EABS	8.0147	9.9708	9.0092
	ARE	19.194	25.346	36.652
	MPSED	198.58	427.29	505.11
	HYBRID	61.167	213.55	333.69
	F Test	0.9908	0.9819	0.9875
	RMSE	0.2762	0.1736	0.1840
	χ^2	0.0714	0.0370	0.0433
Freundlich	SSE	0.0852	0.0783	0.0818
	EABS	9.0002	9.9998	10.000
	ARE	41.736	42.944	41.705
	MPSED	180.72	185.95	180.59
	HYBRID	32.206	31.336	29.654
	F Test	0.8375	0.8772	0.8827
	RMSE	0.2803	0.2675	0.2710
	χ^2	0.0758	0.0627	0.0596

Temkin	SSE	58.302	110.14	218.88
	EABS	8.0031	6.9980	6.0187
	ARE	2.5579	1.4852	1.2111
	MPSED	11.076	6.4311	5.2442
	HYBRID	0.1530	0.0420	0.0351
	F Test	0.9534	0.957	0.9401
	RMSE	6.4662	9.6041	14.230
	χ^2	1.7461	2.7986	6.0417
Halsey	SSE	0.4517	0.4152	0.43393
	EABS	8.9990	9.9998	10.0019
	ARE	18.466	18.929	18.3725
	MPSED	79.960	81.965	79.5553
	HYBRID	5.6246	5.5005	5.1938
	F Test	0.8375	0.8772	0.8827
	RMSE	0.6453	0.6159	0.6240
	χ^2	0.1745	0.1443	0.1371
D-R	SSE	0.9099	1.2889	1.6719
	EABS	9.2793	8.9485	8.8062
	ARE	19.647	17.3603	16.509
	MPSED	85.075	75.1725	71.490
	HYBRID	6.7062	4.6863	4.0837
	F Test	0.4325	0.6397	0.6799
	RMSE	0.8636	1.1048	1.2683
	χ^2	0.3083	0.4116	0.5285

Table 5 *Different statistics function parameters for the adsorption of Basic Green 4 onto fireclay-MnO_2 nanocomposite material*

Model	**G^2**			**AIC_C**		
	30 °C	**45 °C**	**60 °C**	**30 °C**	**45 °C**	**60 °C**
Langmuir	0.0447	0.0951	0.0244	11.6177	-2.2763	-2.5096
Freundlich	0.0702	0.0593	0.0556	7.2800	6.0172	6.6765
Temkin	1.7128	2.9109	6.8302	105.205	114.7477	125.0487
Halsey	0.1646	0.1360	0.1267	32.3010	31.0381	31.6975
DR	0.2715	0.4976	0.4976	42.8046	48.0275	51.9306

Table 6 *Comparison of Basic Green 4 adsorption capacity of fireclay MnO_2 nanocomposites with other reported low-cost adsorbents*

Adsorbent	Adsorption Capacity (mg/g)	Reference
Bentonite	95.15	[37]
Activated clay	91.23	[38]
Fireclay and MnO_2 composites	76.41	Present study
Montmorillonite clay and iron oxide composites	69.11	[39]
Palygorskyte	48.39	[40-41]

The other parameters in error analysis like EABS, ARE, MPSED and HYBRID indicate the data for the adsorption process fit into different isotherms in the order Temkin >DR >Halsey> Freundlich> Langmuir. These results show that the adsorption of

Basic green 4 fit well to Temkin followed by Langmuir isotherm. The F test and AICc results also indicate the adsorption process is favorable for Langmuir.

4. Conclusion

The adsorption of Basic green 4 was influenced by several operational factors and the adsorption capacity of the adsorbent increased with increase in temperature. The experimental data are well fitted with Langmuir and Temkin isotherm dominate almost exclusively for the error function models. The error analysis gives a satisfactory fit to Temkin isotherms. The smaller molecular mass of the dye adsorbed by the nanocomposites is represented by the Langmuir and Temkin isotherm models. The maximum monolayer adsorption capacity achieved was 76.41mg/g in this study. The lower capacity of the system using molecular weight dyes on nanocompositefavour for Temkin isotherm. The statstics also give the goodness of fit to Langmuir isotherm.

References

[1]. M. Bahram, R. Talebi, A. Naseri, S. Nouri, 2014,Journal of Science, **41**, 1230 .
[2]. E. Forgacs, T. Cserhati, G. Oros,2004, Environment International, **30**, 953
[3]. T. Robinson, G., McMullan, R. Marchant, P. Nigam, 2001,Bioresource Technology, **77**, 247 .
[4]. T. Shichi, K. Takagi, 2000,Clay minerals as photochemical reaction fields. Journal of Photochemistry and Photobiology C: Photochemistry Reviews, **1**, 113
[5]. G.J. Churchman, 2002Applied Clay Science, **21**, 177.
[6]. C. Breen, 1999, Applied Clay Science, **15**, 187.
[7]. A. Radian, Y.G. Mishael, 2008, Environmental Science & Technology, **42**, 1511.
[8]. D. Zadaka, S. Nir, A. Radian, Y.G. Mishael,2009, Water Research, **43**, 677.
[9]. R. Srinivasan, 2011, Advances in Application of Natural Clay and Its Composites in Removal of Biological, Organic, and Inorganic Contaminants from Drinking Water, Volume. 872531, 17.
[10]. L. Singoredjo, R. Korver, F. Kapteijn, J. Moulijn,1992, Applied CatalysisB, **1**, 297.
[11]. L. Wang, Y. Liu, M. Chen, Y.Cao, H. He, K. Fan, 2008,Journal of Physical Chemistry C, **112** (17), 6981 .
[12]. K.K.H. Choy, J.F. Porter, G. McKay,2004a , Chemical Engineering Journal, **98**, 255 .
[13]. K.K.H. Choy, J.F. Porter, G. McKay, 2005bChemical Engineering Journal, **103**, 133 .
[14]. I. Langmuir, 1918,Journal of the American Chemical Society, **40**, 1361 .
[15]. U. Freundlich, 1906, Zeitschrift fur PhysikalischeChemie. **57**, 385 .
[16]. M.I. Temkin, 1940,V. Pyzhev, Actaphysicochimica U.R.S.S, **12**, 327 .
[17]. M.I. Temkin, 1940,V. Pyzhev, Actaphysicochimica U.R.S.S, **12**, 217 .
[18]. M. Dubinin, L. Radushkevich, 1947,Chemistry Zentr. **1**, 875 (1947).
[19]. M.M. Dubinin, L.V. Radushkevich, Dokl. Akad. Nauk. SSSR **55**, 327 .
[20]. G. Halsey, 1948, Journal of Chemical Physics, **16**, 931 .
[21]. C. Wei, H. Pang, B. Zhang, Q. Lu, S. Liang, F. Gao, 2013,Scientific Reports, **3**, 2193.
[22]. C. A. Basker, 2006,Journal of Hazardous Material, **135B**, 232 .
[23]. T.S. Malarvizhi, T. Santhi, 2012,Research on Chemical Intermediates, 1-22 .
[24]. K.R. Hall, 1966,Industrial & Engineering Chemistry Fundamentals, **5**, 212 .
[25]. S. Arivoli, B. R.Venkatraman, T.Rajachandrasekar, M. Hema, 2007,Research Journal of Chemistry and Environment,**17**, 70 .
[26]. M. Hema, S. Arivoli,.2008, Journal of Applied Sciences and Environmental Management, **12**(1), 43 .
[27]. C. Namasivayam, N. Muniasamy, K. Gayatri, M. Rani, K. Ranganathan, 1996,.Bioresource Technology, **57**, 37 .
[28]. M.C. Ncibi, S. Altenor, M. Seffen, F. Brouers, S. Gaspard, 2008,Chemical Engineering Journal, **145**, 196 .
[29]. N. Tichaona, H. Olindah,2013, International Journal of Advances in Engineering & Technology, **6**, 128 .
[30]. C. Aharoni, M. Ungarish,1977,Journal of the Chemical Society, Faraday Transactions 1: Physical Chemistry in Condensed Phases. **73**, 456 .
[31]. Y. Khambhaty, K. Mody, S. Basha, B. Jha, 2009,Chemical Engineering Journal, **145**, 489.
[32]. M.M. Dubinin,1960, Chemical Reviews. **60**, 235 .
[33]. A.M. Vargas, A.L. Cazetta, M.H. Kunita, T.L. Silva, V.C. Almeida,2011, Chemical Engineering Journal, **168**, 722
[34]. M. Hadi, R. Mohammad, Samarghandi, G. McKay, 2010,Chemical Engineering Journal, **160**, 408 .
[35]. J.C.Y. Ng, W.H. Cheung, G. McKay,2002, Journal of Colloid and Interface Science, **255**, 64 .
[36]. S.J. Allen, Q Gan, R. Matthews, P. A. Johnson, 2003,Bioresource Technology, **88**, 143 .
[37]. Y. Liu, Y. Kang, B. Mu, Wang, 2014,Chemical Engineering Journal, **237**, 403 .
[38]. C.H. Weng, Y.F. Pan, 2007,Journal of Hazardous Materials, **144**, 355 .
[39]. L. Cottet, C.A.P. Almeida, N. Naidek, M.F. Viante, M.C. Lopes, N.A. Debacher,2014,Applied Clay Science, **95**, 25
[40]. H. Chen, J. Zhano, A.Zhong, Jin, 2011b,Chemical Engineering Journal, **174**, 143 .
[41]. H. Chen, J. Zhao, J. Wu, G. Dai, 2011a,Journal of Hazardous Material, **192**, 246 .